

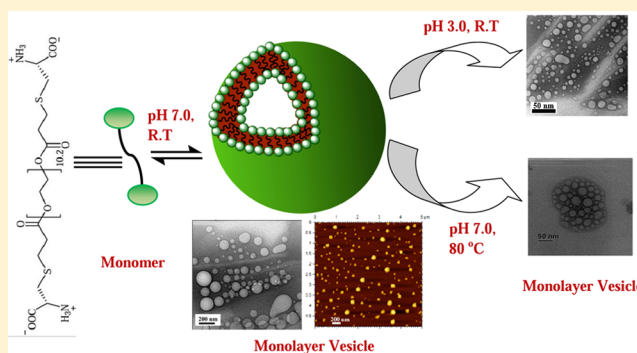
An Unconventional Zwitterionic Bolaamphiphile Containing PEG as Spacer Chain: Surface Tension and Self-Assembly Behavior

Rita Ghosh and Joykrishna Dey*[✉]

Department of Chemistry, Indian Institute of Technology, Kharagpur 721 302, India

Supporting Information

ABSTRACT: Monolayer lipid membrane formation based on self-assembly of bolaamphiphiles containing hydrophobic spacer are well-established in the literature, but monolayer vesicle formation by so-called hydrophilic poly(ethylene glycol) (PEG) spacer has not been reported to date. Here, a novel L-cysteine-derived bolaamphiphile with PEG as spacer has been developed and characterized. The interfacial properties and the solution behavior of the amphiphile were investigated in pH 7.0 at 25 °C. The self-assembly properties of the bolaamphiphile in aqueous buffer were investigated by using different techniques, such as surface tensiometry, fluorescence spectroscopy, UV–vis spectroscopy, isothermal titration calorimetry, dynamic light scattering, transmission electron microscopy, and atomic force microscopy. Surprisingly, despite having so-called polar spacer in between two polar head groups, it exhibits formation of microstructures in aqueous buffer as well as in water at 25 °C. The molecule undergoes self-organization leading to the formation of monolayer vesicles with hydrodynamic diameters between 100 and 250 nm in a wide range of concentration. The thermodynamic parameters clearly suggest that the aggregate formation is mainly driven by the hydrophobic effect. The monolayer vesicles were found to form at a very low concentration (≥ 0.63 mM) and within a wide pH range (2–10). The vesicles exhibit excellent shelf life at physiological temperature.



1. INTRODUCTION

Conventional bolaamphiphiles are two-headed bipolar amphiphiles consisting of two hydrophilic head groups separated by a hydrophobic spacer.^{1–6} The two hydrophilic head groups in a bolaamphiphile can be charged or uncharged and can even be identical to or different from each other. On solid surface bolamphiphiles are known to self-associate into monolayers.^{7–11} On the other hand, bolaamphiphiles form different types of self-assemblies, including micelle, monolayer lipid membrane (MLM), vesicles, tubes, helical structures, multilayers, and nanofibers in aqueous solution.^{12–19} However, it has been found that the basic thermodynamic properties of bolaamphiphiles, including critical micelle concentration (cmc) and micellization free energy, are not just twice that of the corresponding conventional surfactant having just half of its length.

Bolaamphiphiles have been shown to have enough potential in effective drug as well as gene delivery. Therefore, they are now widely employed in formulating stable nanocarriers systems. In fact, there are many reports on chemical properties of bolaamphiphiles and their effects on self-assembly behavior.^{20–22} Thus, after 30 years of initial development, bolaamphiphiles have now become a new field of research to formulation chemists and biologists. Bolaamphiphiles can also serve as important structural blocks of micelles, vesicles, and other nanostructures for biomedical applications as depicted by

archaeosomes. A number of reports on bolaamphiphiles depict that they can be used as the potential candidates for the formulation of nanovehicles for targeted delivery of drugs and genes. Extensive research is also going on to assess their safety profile to establish them as safe excipients for pharmaceutical applications.

Despite numerous reports on the aggregation behavior and biomedical applications of bolaamphiphiles containing hydrocarbon chains, steroids, porphyrines, etc., until now there is not a single report on bolaamphiphile bearing poly(ethylene glycol) (PEG) as spacer. We all know about the versatile uses of PEG in biomedical and pharmaceutical applications.^{23,24} Since PEG is flexible in nature, nonreactive, less toxic, and water-soluble, it shows versatile properties. Moreover, very high water solubility of PEG at moderate temperatures leads to its enormous applications in drug delivery, biomedical applications, surfactant chemistry, and osmotic stress methods.²⁵ Indeed, PEGs having low molecular weight ($M_n < 1500$ Da) are generally considered hydrophilic.²⁶ However, recently, work from this laboratory has demonstrated self-assembly formation PEG-containing single-tailed surfactants where PEG itself acts as the hydrophobic tail.^{27–30} In this work, we were interested in developing a first-

Received: June 4, 2017

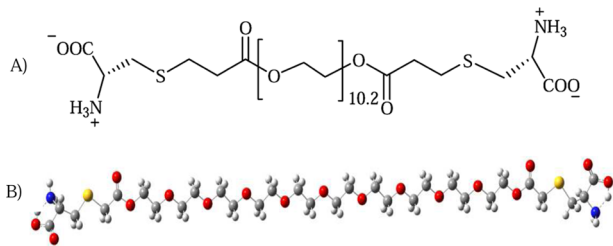
Revised: July 12, 2017

Published: July 13, 2017

in-class bolaamphiphile containing PEG backbone as the spacer. It will be very interesting to see whether the PEG-containing bolaamphiphile can form aggregates in solution. If yes, then it would be interesting to see what kind of aggregate they will form in aqueous solution.

Therefore, in this work, we have developed a pH-sensitive zwitterionic bolaamphiphile, poly(ethylene glycol) di(propionyl cysteine) (PEGDPC) (see Chart 1 for structure), bearing PEG

Chart 1. (A) Molecular Structure of the Amphiphile (PEGDPC) and (B) Energy-Minimized Structure of the Amphiphile in Solution Phase (Water) (Gray: C; White: H; Red: O; Blue: N; Yellow: S)



as spacer and L-cysteine as the polar head groups. It was intended to examine if there is any micelle formation by this new class of amphiphile. Zwitterionic bolaamphiphile with PEG spacer is advantageous because the amphiphile is pH-sensitive. Also, since both PEGs and L-cysteine are biocompatible and eco-friendly, their self-assembled structures in aqueous medium can have potential applications in drug delivery. Therefore, self-assembly properties of this amphiphile were investigated in pH 7.0 buffer at 25 °C. The cmc of the amphiphile and micropolarity and microviscosity of the nanostructures were estimated by the fluorescence probe technique. The energetics of the self-assembly process was investigated by isothermal titration calorimetry (ITC). The standard free energy change (ΔG°_m) and standard enthalpy change (ΔH°_m) of micellization were measured to understand the nature of molecular interactions. The size and shape of the aggregates were determined by using methods, including dynamic light scattering (DLS), transmission electron microscopy (TEM), and atomic force microscopy (AFM). The stability of the aggregates with respect to aging, concentration, solution pH, and temperature was examined.

2. EXPERIMENTAL SECTION

Materials. Poly(ethylene glycol) diacrylate (M_n 575), *N*-phenyl-1-naphthylamine (NPN, 98%), pyrene (Py, 99%), 1,6-diphenyl-1,3,5-hexatriene (DPH, 98%), and D₂O (99.6 atom % D) were obtained from Sigma-Aldrich (Bangalore, India). For further purification, the fluorescent probes were recrystallized from acetone–ethanol mixture two times before use. Fluorescence excitation spectra of the probes were recorded to confirm purity. L-Cysteine was obtained from Lab Chem (Kolkata, India) and was used without further purification. Sodium dihydrogen phosphate (NaH₂PO₄) and disodium monohydrogen phosphate (Na₂HPO₄) obtained from SRL (Mumbai, India) were of analytical grade. Methanol and triethylamine (TEA, 98%) purchased from Merck (Mumbai, India) were further dried for use in synthesis. Milli-Q water (18 MΩ cm) was used for the preparation of aqueous solutions.

The amphiphile PEGDPC was synthesized following a method reported earlier by our group.^{29,30} The details of synthetic procedure are available in the Supporting information.

NMR Measurements. All 1D (¹H and ¹³C) and 2D NMR spectra were recorded on a Bruker (600 MHz) NMR spectrometer. D₂O solvent was used as the chemical shift reference for mode locking.

Surface Tension Measurements. Surface tension (γ) measurements were carried out with a surface tensiometer (GBX 3S, France) applying the Du Nüoy ring method. Before each measurement, the instrument was calibrated by measuring the surface tension of Milli-Q water (18 MΩ cm). The γ value was measured by successive addition of aliquots of PEGDPC stock solution to a 10 mL phosphate buffer (pH 7.0) solution. Before each measurement the solution was equilibrated for 10 min at 25 °C. Each measurement was repeated three times to minimize any error. A JULABO MC water-circulating bath with a temperature accuracy of ± 0.1 °C was used for temperature control.

Steady-State Fluorescence Measurements. The fluorescence spectra of NPN and DPH probes were recorded on a PerkinElmer LS-55 luminescence spectrometer equipped with a temperature-controlled cell holder. A SPEX Fluorolog-3 (FL3-11, USA) spectrophotometer was used to measure fluorescence emission spectra of Py. For fluorescence measurements surfactant solutions of required concentrations were prepared in pH 7.0 buffer and were equilibrated for about 30 min prior to measurement. The final probe concentrations (Py and DPH) were kept at 1 μ M. Py solutions were excited at 335 nm, and emission spectra were recorded in the wavelength range of 350–500 nm using excitation and emission slit widths of 3 and 1 nm, respectively. For fluorescence titration using NPN probe, a saturated solution of NPN in pH 7.0 buffer was used. NPN solutions were excited at 340 nm, and the emission spectra were measured using excitation slit width of 2.5 nm and emission slit width of 2.5–10 nm, depending upon sample concentration. The temperature of the cuvette holder was controlled by a Thermo Neslab RTE-7 circulating bath.

Fluorescence Anisotropy Measurements. Steady-state fluorescence anisotropy (r) of DPH was measured by the PerkinElmer LS-55 luminescence spectrometer equipped with a polarization accessory that uses the L-format instrumental configuration. A Thermo Neslab RTE-7 circulating bath was used for temperature control of the magnetically stirred cuvette holder. The anisotropy was calculated employing the equation

$$r = (I_{VV} - GI_{VH}) / (I_{VV} + 2GI_{VH}) \quad (1)$$

where I_{VV} and I_{VH} are the fluorescence intensities when the emission polarizer is oriented parallel and perpendicular to the excitation polarizer, and $G (= I_{HV}/I_{HH})$ is the instrumental grating factor. The software supplied by the manufacturer automatically determined the G factor and r . In all measurements, the r value was recorded over an integration time of 10 s, and an average of five readings was accepted as the r value. A stock solution of 1 mM DPH was prepared in super dry methanol. The final concentration of DPH was maintained at 1 μ M by addition of an aliquot of the stock solution. Variable temperature anisotropy measurements were performed in the temperature range 25–75 °C. The sample was excited at 350 nm, and the emission intensity was followed at 450 nm using excitation and emission slit width of 2.5 nm and 2.5–10.0 nm, respectively. A 430 nm emission cutoff filter was employed to reduce the effect of scattered and stray radiation. The fluorescence measurements started 30 min after sample preparation.

Time-Resolved Fluorescence Measurements. The fluorescence lifetime (τ_f) of DPH probe was measured by an Optical Building Blocks Corporation Easylife instrument that uses a 380 nm diode laser. The time-resolved decay curves were analyzed by single-exponential or biexponential iterative fitting program. Best fitting was judged by the χ^2 value (0.8–1.2) and by the residual plot.

Determination of Microviscosity. The fluorescence lifetime (τ_f) and fluorescence anisotropy (r) of DPH probe were used to determine the microviscosity (η_m) of the aggregates. The η_m value was calculated using Debye–Stokes–Einstein relation:

$$\eta_m = kT\tau_r/v_h \quad (2)$$

where v_h is the hydrodynamic volume (313 \AA^3)³¹ of the DPH probe. The τ_R was calculated using Perrin's equation:

$$\tau_R = \tau_f(r_0/r - 1)^{-1} \quad (3)$$

where r_0 ($= 0.362$)³² is the steady-state fluorescence anisotropy of DPH in a highly viscous solvent and τ_f is the measured fluorescence lifetime of DPH in surfactant solution.

Dynamic Light Scattering. The hydrodynamic diameter (d_h) of the aggregates in aqueous media was measured with a Zetasizer Nano ZS (Malvern Instrument Lab, Malvern, U.K.) dynamic light scattering (DLS) spectrometer equipped with a He–Ne laser operated at 4 mW at $\lambda_0 = 632.8 \text{ nm}$. The scattering intensity was measured at $\theta = 173^\circ$ to the incident beam. Surfactant solutions were prepared in pH 7.0 buffer. Before each measurement the solution was filtered through Millipore Millex syringe filter (Triton free, $0.22 \mu\text{m}$). For all light scattering measurements, the temperature was set at 25°C , and the sample was equilibrated inside the DLS optical system chamber for 10 min before the measurement started. The data acquisition was carried out for at least 100 counts, and each experiment was repeated three times.

Zeta-Potential Measurements. The surface zeta (ζ)-potential of the aggregates was determined using the same Zetasizer Nano ZS (Malvern Instrument Lab, Malvern, UK) at 25°C . For each sample, an average of the values of three successive measurements was noted.

Transmission Electron Microscopy (TEM). High-resolution transmission electron micrographs of the specimens were taken on HRTEM (JEOL-JEM 2100, Japan) operating at 200 kV. For sample preparation, $4 \mu\text{L}$ of surfactant solution was dropped on to a 400 mesh carbon-coated copper grid and allowed to stand for 1 min. The excess solution was then blotted with a tissue paper, and the grid was air-dried. The specimens were kept in vacuum desiccators until before measurement. Each measurement was repeated at least three times to check the reproducibility.

For cryo-TEM measurements, 3 and 10 mM PEGDPC solutions were prepared in pH 7.0 buffer. Specimen preparation was done in a controlled environment vitrification system (CEVS). The specimens were prepared in a chamber at 100% relative humidity (Cryoplunge 3) in order to keep surfactant concentration fixed. $5 \mu\text{L}$ of the sample solution was applied via the side port of the Vitrobot directly onto the carbon-coated side of the Formvar carbon-coated perforated polymer film TEM grid held by tweezers inside the chamber by using a pipet. The excess solution was then blotted with a filter paper wrapped on a metal trip to thin the drop into a film the thickness of which was less than 300 nm. The grid was then plunged into liquid ethane at its freezing point (-170°C) cooled by liquid nitrogen. Until imaging, the vitrified specimens were kept under liquid nitrogen, and the temperature was maintained at -170°C . Cryo-specimens were imaged in JEM-2100F transmission electron microscope (JEOL, Japan), operated at 200 kV, using a Gatan 655 (Gatan, Pleasanton, CA) cooling holder and transfer station. Specimens were equilibrated in the microscope below -170°C . To nullify the electron beam radiation damage, the specimens were investigated under low-dose intensity. The images were recorded at a nominal under focus to enhance phase contrast and were acquired digitally by CCD cameras (Gatan, Pleasanton, CA), using the Digital Micrograph software (Gatan UK, Abingdon, UK).

Atomic Force Microscopy (AFM). AFM measurements were conducted by a Nanoscope IIIA from Digital Instruments in tapping mode under ambient conditions. For the sample preparation, one drop of 10 mM PEGDPC solution was placed on a clean mica surface. The specimen was then dried in air overnight.

Gauss View Analysis. To get the energy-minimized monomeric structures of the amphiphile in solution state (water), the theoretical study was performed. All the calculations were done using the Gaussian 09 software package.³³ The geometries were optimized with the spin-unrestricted formalism using B3LYP functional and 3-21G* basis set. The polarized continuum model (PCM) was used to model the solvation effects of water.

Isothermal Titration Calorimetry (ITC). The thermometric measurements were performed by use of an isothermal titration

calorimeter (Microcal iTC₂₀₀, U.S.A.) at 25°C . For the measurements, concentrated surfactant stock solution (5 mM) was taken in a microsyringe of capacity $40 \mu\text{L}$ and was added in multiple steps to pH 7.0 buffer kept in the calorimeter cell of capacity $200 \mu\text{L}$ under constant stirring conditions. The stirring speed was set at 400 rpm. The reference cell contained pH 7.0 buffer. The thermogram of the heats of dilution by stepwise addition of the surfactant solution was recorded. Each run was performed twice to check reproducibility. The calculation of heat changes was performed with the help of ITC software provided by the manufacturer.

3. RESULTS AND DISCUSSION

Surface Tension. Amphiphilic molecules are known to self-organize at the air/water interface which is indicated by the reduction of γ value of water. The surface tension of the aqueous solutions of PEGDPC at different concentrations was measured at pH 7.0 and 25°C . The decrease of γ value upon increase of PEGDPC concentration (C_s) (Figure 1) suggests

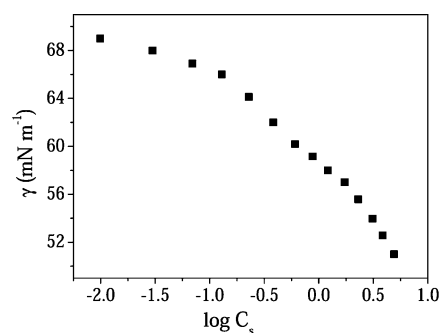


Figure 1. Plot of surface tension (γ) versus $\log C_s$ (M) of PEGDPC in pH 7.0 at 25°C .

amphiphilic character and spontaneous adsorption of PEGDPC molecules at the interface. The surface activity of an amphiphile as usually measured by the pC_{20} value ($-\log(\text{concentration of the amphiphile required to lower } \gamma \text{ value of water by 20 units})$) was observed to be ~ 2.3 . Since for good surfactants the pC_{20} value is ≥ 3 , PEGDPC can be considered as a reasonably good surfactant.^{34,35} Interestingly, unlike conventional surfactants, the plot does not show any break followed by a plateau in the investigated concentration range. However, a dent in the curve can be seen at C_s of about 0.5 mM, which may be taken as the cmc value. The reduction of γ value at higher concentrations ($> \text{cmc}$) can be attributed to formation of larger aggregates. Similar behavior has already been reported in the literature for other surfactants.^{29,30}

Self-Assembly Studies. NPN has been extensively used as an efficient fluorescent probe as it shows a large spectral shift along with a huge increase of intensity upon incorporation into the hydrophobic microdomains of the self-assembled microstructures.³⁶ In the presence of PEGDPC the fluorescence emission maximum (λ_{max}) of NPN exhibits a 55 nm blue-shift and about 10 times enhancement of fluorescence intensity relative to that in pH 7.0 buffer (Figure 2a). The large blue-shift of λ_{max} of NPN suggests its encapsulation within less polar environment of the microstructures formed by PEGDPC molecules in aqueous solution. In addition, the enhancement of the fluorescence intensity indicates a viscous microenvironment of the NPN probe. The plot showing variation of the spectral shift $\Delta\lambda$ ($= \lambda_{\text{max}}(\text{water}) - \lambda_{\text{max}}(\text{surfactant})$) of the NPN probe with C_s is depicted in Figure 2b. The sigmoid plot corresponding to a two-state process clearly suggests existence

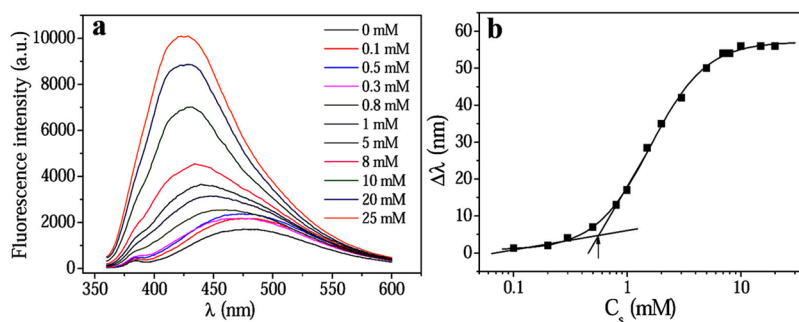


Figure 2. (a) Representative fluorescence emission spectra of NPN in pH 7.0 buffer in the presence of different concentrations of PEGDPC (C_s). (b) Plot of variation of spectral shift ($\Delta\lambda$) of NPN probe in phosphate buffer (20 mM, pH 7.0) with the change in C_s at 25 °C.

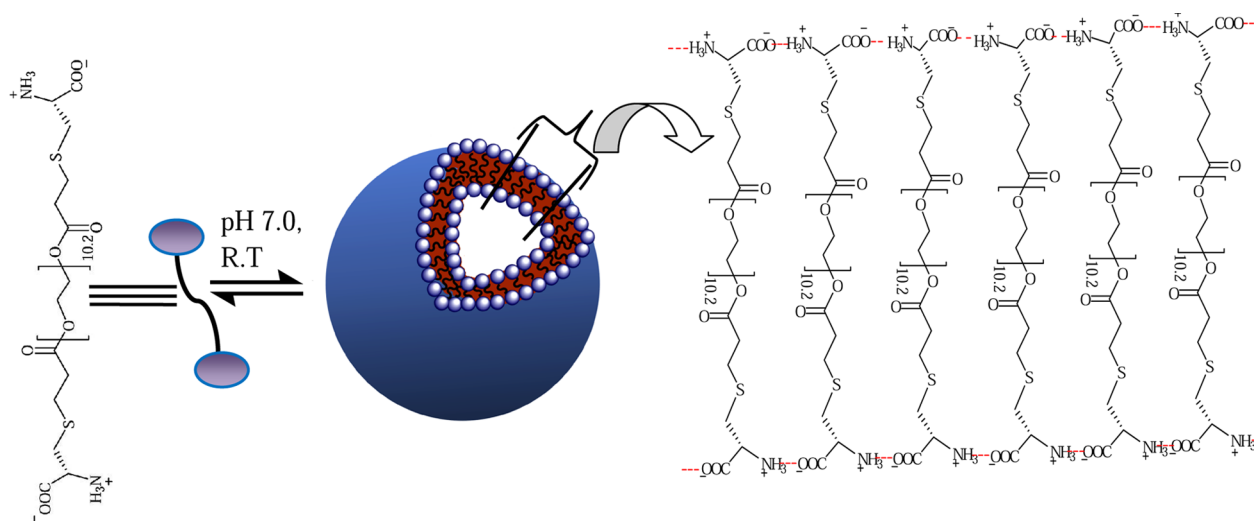


Figure 3. Schematic representation of monolayer vesicle structure formed by the monomers.

of equilibrium between surfactant monomers and self-assembled aggregates. The cmc value (0.60 ± 0.04 mM) obtained from the onset of rise of $\Delta\lambda$ is almost equal to the value obtained from surface tension plot.

The microenvironment of the aggregates was also investigated using Py probe to estimate micropolarity and thereby to have an idea about the nature of the aggregates. The ratio of the intensities of first (I_1 , 374 nm) and third (I_3 , 384 nm) vibronic bands in the Py fluorescence spectrum is usually used as an index of apparent polarity of the medium.³⁷ The fluorescence emission spectra of Py measured in pH 7.0 buffer at different C_s are depicted in Figure S4. In pure buffer medium, the I_1/I_3 ratio has a value of 1.81. But the ratio falls off with increasing C_s , and the limiting value reaches to 1.48 ± 0.03 at $C_s = 20$ mM, indicating formation of microstructures with micropolarity less than that of water. However, this micropolarity index is higher than that of aggregates formed by the single PEG tail surfactant with the L-cysteine head group.²⁹ The micropolarity value corresponds to the polarity of ethylene glycol.³⁸ In pH 3.0 buffer, however, the decrease of the I_1/I_3 ratio is much larger, and the limiting value (1.38 ± 0.04) is reached at 20 mM PEGDPC. That is, when the head groups become cationic ($-\text{NH}_3^+$) in nature, the microenvironment of the aggregates becomes less polar. This suggests that the Py or NPN probes are solubilized within the microdomains of the aggregates constituted by the PEG spacer of the amphiphile.

Further, in order to investigate whether there is any structural change of the aggregates with increase of PEGDPC

concentration, steady-state fluorescence anisotropy (r) of DPH probe was measured. As reported in the literature, the rigidity of the microenvironments of aggregates is manifested by the r value of DPH probe.^{32,39} A high r value (>0.14) indicates viscous microenvironment. Thus, the high r value (0.185 ± 0.003) of DPH in 20 mM PEGDPC solution indicates that the microenvironment of the probe molecules is very rigid and is constituted by tight packing of PEG chains.⁴⁰ The microviscosity (η_m) was calculated from the steady-state r value (0.185) and fluorescence lifetime ($\tau_f = 5.28 \pm 0.10$ ns) of the DPH probe using the Debye–Stokes–Einstein relation.³² The η_m value thus obtained is ca. 70.14 mPa·s, which is much higher than those of conventional surfactant micelles.³¹ The plot (Figure S5) showing variation of r value with the increase of C_s shows an increase of η_m of the aggregates with the increase of C_s above the cmc. This can be attributed to formation of aggregates with core constituted by tighter packing of the PEGDPC molecules.

On the basis of the results of fluorescence probe studies, we propose vesicle formation by the amphiphiles as shown by the cartoon pictures depicted in Figure 3. The vesicle wall is constituted by the monolayer arrangement of the PEGDPC molecules. The constitution of vesicle membrane was also confirmed by 2D NOESY analysis. The NOESY analysis reveals through-space interactions among the protons of close proximity in a molecule as well as in a complex of molecules.^{41,42} The distance of two specific protons ($^1\text{H}-^1\text{H}$) in a NOESY spectrum predominantly controls the intensity

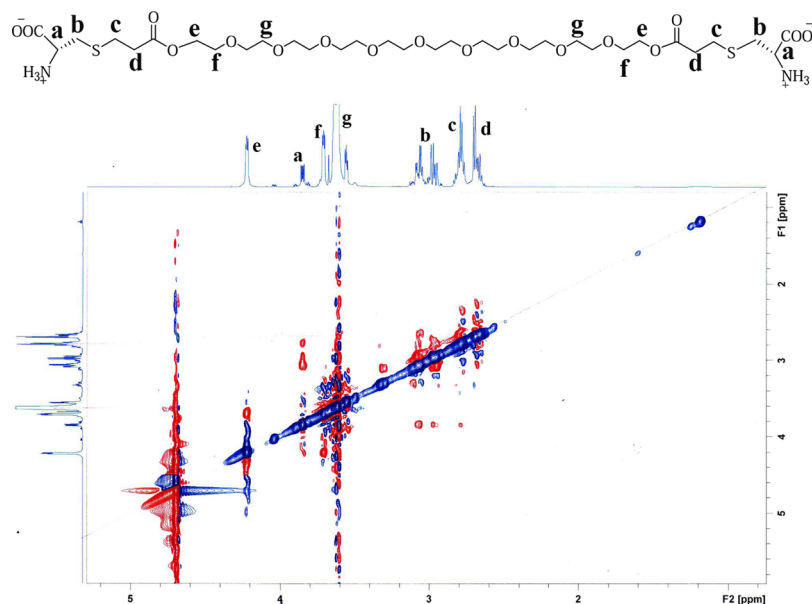


Figure 4. 2D NOESY spectrum of 1 mM PEGDPC in D₂O (aggregated state).

(volume) of cross-peak formed by the protons. The NOESY spectrum of 1 mM PEGDPC solution (in D₂O) as depicted in Figure 4 shows mostly diagonal peaks that arise from the interactions of the nearby H atoms in the same molecule. It is evident from Figure 4 that along with diagonal interactions a number of key cross interactions can also be observed. The interactions among g ↔ a, b, c, d, e, f protons imply the intermolecular interactions among the PEG chains. Further, the interactions among a ↔ b, c, d and b ↔ c, d protons suggest the strong intermolecular interactions among the head groups. All these strong key cross-peak interactions suggest only monolayer formation after reaching a certain concentration (cmc). These cross-peaks signify the spatial proximity of the surfactant in the self-assembled aggregates. This means that the monolayer vesicle is constituted by the PEG spacer of the bolaamphiphile.

Thermodynamics of Aggregate Formation. The ITC method was employed to further investigate the self-assembly behavior of the surfactant and to understand the thermodynamics of aggregate formation. The thermogram along with the titration curve is displayed in Figure 5. The cmc value was obtained from the corresponding differential plot as shown in Figure S6. From this calorimetric titration curve, the ΔH_m° value was directly obtained from the enthalpy difference between final and initial states. The other thermodynamic parameters ΔG_m° and ΔS_m° associated with the micellization process were calculated using the pseudophase separation model.^{43–45} The values of cmc and other thermodynamic parameters evaluated from the data presented in Table 1. The spontaneity of vesicle formation is confirmed by the large negative values of ΔG_m° as well as by the large positive values of ΔS_m° . Since the $T\Delta S_m^\circ$ value for the amphiphile is observed to be much larger than that of the ΔH_m° value, it clearly suggests that the spontaneous vesicle formation is an entropy-driven process. The essence of entropy-driven process is the hydrophobic interaction. The release of water molecules around the PEG tails contributes to the entropy rise which is beneficial for the self-assembly process. This means that the hydrophobic effect plays an important role in vesicle formation.

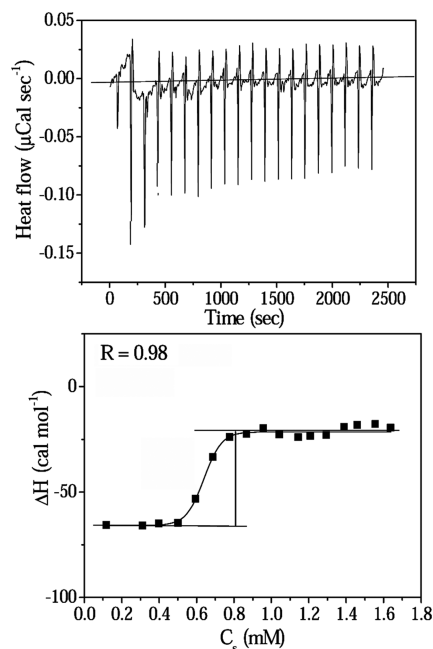


Figure 5. Thermogram (upper panel) and plot of variation of enthalpy change (ΔH) with surfactant concentration (C_s) at 25 °C; concentration of surfactant stock solution was 5 mM.

Table 1. Critical Micelle Concentration (cmc), Standard Gibbs Free Energy Change (ΔG_m°), Standard Enthalpy Change (ΔH_m°), and Standard Entropy Change (ΔS_m°) for the Self-Assembly Formation in Aqueous Buffered Solution (pH 7.0) by PEGDPC at 25 °C

cmc (mM)	ΔG_m° (kJ mol ⁻¹)	ΔH_m° (kJ mol ⁻¹)	ΔS_m° (J K ⁻¹ mol ⁻¹)	$T\Delta S_m^\circ$ (kJ mol ⁻¹)
0.63 (±0.02)	-18.26	0.19 (±0.1)	61.91	18.45

In other words, the PEG chain of the bolaamphiphile behaves like a hydrocarbon chain. However, when the thermodynamic data for the vesicle formation by PEGDPC are compared with those of the corresponding single-headed zwitterionic amphi-

phile, it is found that the aggregate formation is more feasible in the latter.²⁹

Hydrodynamic Size and Shape of Aggregates. DLS measurements were performed to determine mean hydrodynamic diameter (d_h) of the aggregates formed at different concentrations and pH. The histograms in Figure 6 represent

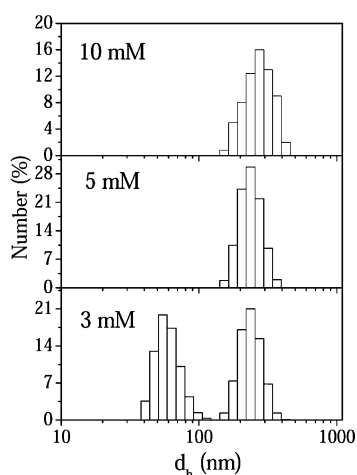


Figure 6. Concentration-dependent size distribution profiles of the aggregates formed by PEGDPC in pH 7.0 buffer at 25 °C.

the number distribution graphs for the amphiphile at different concentrations. It is observed that the aggregates formed in pH 7.0 have bimodal size distributions. The aggregates are found to have mean d_h much larger than that of small spherical micelles. The size distribution histograms presented in Figure 6 clearly suggest formation of vesicles having d_h value in the range of 50–250 nm. As expected at higher concentrations (5 and 10 mM), a monomodal size distribution with a mean d_h of ca. 250 nm is observed. This indicates that size of the vesicles remains almost unchanged when surfactant concentration is increased. The surface potential of the vesicles in 3 mM PEGDPC solution was also measured and the data are collected in Table S1. Slightly negative ζ -potential value (-5.2 mV) of the vesicles in neutral pH (~ 6.0 – 7.0) clearly suggests that the L-cysteine head group of the bolaamphiphile is oriented toward bulk water.

Further HRTEM images of PEGDPC solutions of two different concentrations were taken to visualize the shape of the microstructures formed in aqueous solution. The TEM images as shown in Figure 7 reveal the existence of spherical vesicles with an aqueous core. It is important to note that the surfactant solution in pure water also exhibits formation of vesicular structures (Figure S7). The vesicle diameters (50–150 nm) in 3 mM surfactant solution as seen in the micrographs are slightly less than the values obtained by DLS measurements, which is due to drying of the sample. A very careful insight into the vesicular pictures (Figure 7b) reveals that the thickness of the vesicle wall is ~ 4 nm, which is almost equal to the length of the spacer PEG chain (40.51 Å) as obtained from the Gaussview model of the molecule. The microscopic investigations thus confirm the existence of monolayer vesicle formation in both dilute and concentrated surfactant solution. Since the PEG chain is relatively short, monolayer lipid membrane (MLM) formation is much more favorable than bilayer lipid membrane (BLM) formation. This is because for BLM formation the

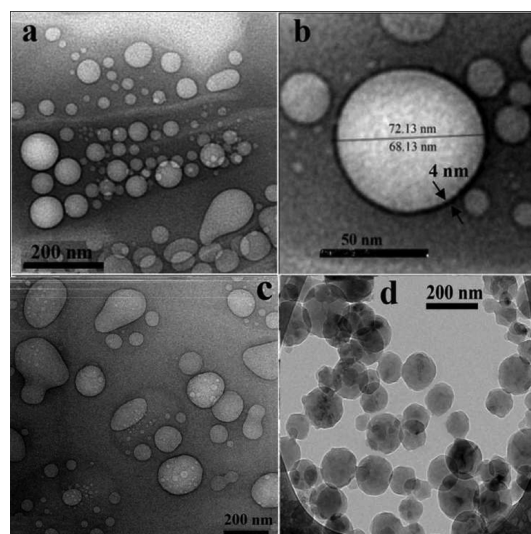


Figure 7. Unstained HRTEM images of PEGDPC in pH 7.0 buffer: (a, b) 3 mM and (c) 5 mM. Cryo-TEM image of (d) 3 mM PEGDPC in pH 7.0 buffer.

molecule has to be bent in a U-shape, which is energetically unfavorable.

To illustrate the molecular packing of PEGDPC in the vesicle wall, the aggregates were further characterized by AFM in a dehydrated state. As shown in Figure 8, the tapping-mode AFM image of 10 mM PEGDPC solution reveals spherical aggregates with diameters of 80–220 nm. This is in good agreement with the result obtained from TEM and DLS measurements. The section analysis profile of a selected aggregate is shown in Figure 8. The collapsed aggregate height was observed to be ~ 8 nm. This means the average wall thickness of the hollow sphere is about 4 nm, which is almost equal to the spacer length of PEGDPC (40.51 Å) calculated using the Gaussview model. This coincidence indicates that the vesicle wall is composed of only one monolayer of PEGDPC molecules rather than the usually observed bilayer structure in vesicles of phospholipids. Considering its similarity to a symmetric bolaamphiphile with short chain, PEGDPC could not adopt a U-bent shape but spanned the wall to form a “monolayer-like” structure.

As the HRTEM and AFM methods are associated with the drying of the sample, the images might appear as artifacts. Therefore, in order to rule out the possibility of any artifact in the HRTEM and AFM images, cryo-TEM measurements were performed at two different concentrations. The cryo-TEM image of the 3 mM PEGDPC solution is shown in Figure 7d. The image clearly reveals existence of vesicles having outer diameters in the range of 120–180 nm. Also, no significant or only a slight increase of vesicle diameter was observed in 10 mM PEGDPC solution (Figure S7). Thus, the results are consistent with the results of DLS, HRTEM, and AFM measurements.

Further to demonstrate the presence of aqueous core in the vesicular aggregate, encapsulation of a hydrophilic dye, methylene blue (MB), was attempted. For the dye entrapment study, 50 mg of PEGDPC (to make 60 mM stock solution) with 100 μ L of 2 mM MB in methanol was mixed and dried slowly in a RB flask by use of a rotavapor to make a thin film. The flask was kept overnight in desiccators for complete evaporation of the solvent. The film was then rehydrated with a small amount of buffer solution for overnight. The rehydrated

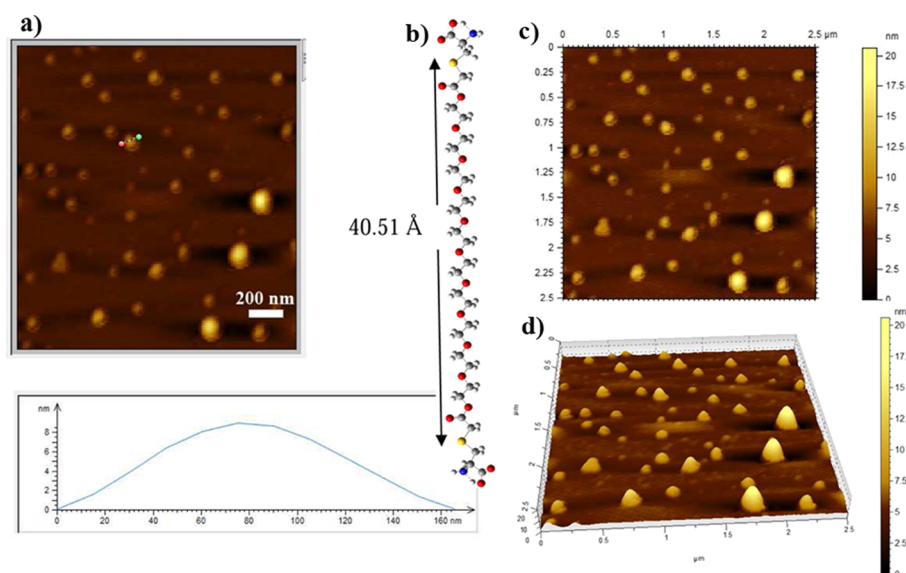


Figure 8. (a) AFM height image, (b) the energy-minimized structure of PEGDPC in solution phase (water) showing the spacer length, (c) AFM image with scale bar, and (d) 3D sectional analysis of PEGDPC solution (10 mM, pH 7.0) on mica.

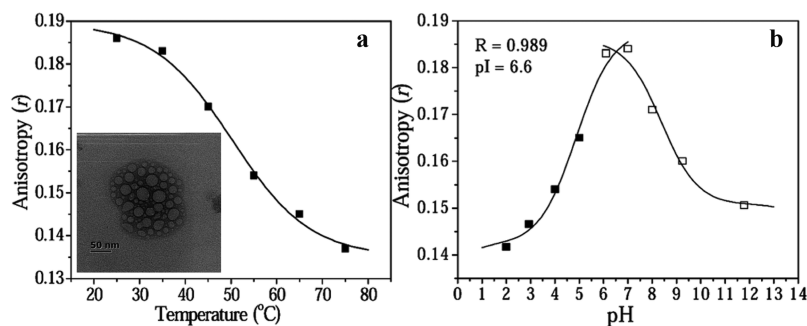


Figure 9. Plots of variation of fluorescence anisotropy (r) of DPH as a function of (a) temperature (inset: TEM image at 80 °C) and (b) pH.

suspension was vortexed for 30 min followed by dilution with pH 7.0 buffer to attain 0.1 mM MB ($\lambda_{\text{max}} = 665$ nm). The resulting solution (2 mL) was then loaded into a column packed with Sephadex G-75 (25 cm height and 1.2 cm diameter) pre-equilibrated in the eluting buffer. The elution was carried out using pH 7.0 buffer, and the eluent was collected in 2 mL fraction each. The vesicular suspensions eluted just after the void volume. However, the filtration was continued to gel filter all the free MB dye. The absorbance for all the fractions was measured at 665 nm. The data are plotted against the elution volume as shown in Figure S8. The encapsulation was confirmed by the characteristic UV spectrum of MB in water. The peak with low absorbance corresponds to the vesicle entrapped dye molecule, whereas the peak of very high absorbance corresponds to the free dye. It was found that approximately 1.75% of the total dye was entrapped into a small initial portion containing vesicles. This study clearly demonstrates that the vesicles contain inner aqueous pool which can entrap water-soluble drugs.

Stability of the Vesicles. Temperature has an important factor of self-assembly formation, and it also affects the size and shape of self-assembled aggregate. Since the microenvironment of the vesicle membrane formed by the PEG spacer is slightly polar in character, it can be concluded that the PEG chains in the membrane are partially hydrated. Thus, heating of the PEGDPC solution is expected to cause dehydration of the PEG

chains and hence change the membrane rigidity. The fluorescence anisotropy of DPH probe was used to determine the phase transition, if any, of the vesicle membrane. Figure 9a depicts the variation of r with temperature. As seen, the r value decreases with the increase of temperature, but the limiting value of r lies in the vesicular range, even at 80 °C. The existence of vesicle phase at 80 °C was confirmed by the TEM image depicted in the inset of Figure 9a. This suggests that the PEG chains become more fluid and hence leaky at elevated temperatures. This is due to weakening of the hydrophobic interactions caused by the thermal motion among PEG chains. The temperature corresponding to the inflection point of the curves can be taken as the melting or phase transition temperature, T_m , of the membrane. The high melting temperature, 48 °C for PEGDPC, clearly suggests that the vesicles are quite stable at the physiological temperature (37 °C).

Since the surfactant headgroup is zwitterionic in nature at pH ~ 6.0 – 7.0 , the stability of the vesicles was studied by varying pH of the medium. The pH-stability measurement was carried out by measuring r of DPH probe in surfactant solutions of different pH. The pH of the solution containing 20 mM PEGDPC was varied from 2 to 12 at 25 °C. Each solution was incubated for 30 min prior to the measurement. Figure 9b shows the variation of r values with the change in pH of the surfactant solution. It is observed that both decrease and

increase of solution pH result in a decrease of r value and show a maximum at pH \sim 6.0–7.0. This suggests that the MLM becomes less rigid at both lower and higher pHs as a result of weakening of the packing of the PEG units. The weak packing of the PEG units results from increased electrostatic repulsion between anionic or cationic head groups of the amphiphiles at the surface. This is associated with the change in ionization equilibrium with pH. The pK_a values for the proton transfer equilibria were obtained from the inflection point of the pH titration curves. The pK_a values thus obtained are 4.8 and 8.4 for cation–zwitterion and zwitterion–anion equilibrium, respectively. The pI value calculated from the respective pK_a value is \sim 6.6, which means that at around neutral pH the surfactants remain in the zwitterionic form and the aggregates exist either as uncharged or weakly charged entities.

In order to investigate the change in vesicle structure with pH, DLS measurements were performed with the PEGDPC solutions of varying pH. The existence of large aggregates in higher as well as in lower pH is confirmed by the size distribution histograms (Figure S9) of the corresponding solution. The size distribution histograms show that with increase or decrease in pH from 7.0 the aggregate size decreases. The aggregate size is highest in pH 7.0 and is consistent with the zwitterionic headgroup of the surfactant at pH 7.0. The existence of vesicles in both lower and higher pHs is demonstrated by the TEM picture (Figure S10) of the respective solution. Indeed, spontaneous vesicle formation was found at pH 3.0 and 10.0. However, the vesicle size becomes smaller in comparison to that in neutral pH, which is consistent with the size distribution histograms in Figure S9. This is due to the cationic and anionic nature of the amphiphile at acidic and basic pH, respectively. In both cationic and anionic forms, electrostatic repulsion among the ionic head groups results in a formation of smaller vesicles.

However, the vesicles were found to be stable enough at all the pHs. The stability of the aggregates is manifested by the surface ζ -potential. A high positive or negative ζ -potential value suggests repulsive interaction among particles and hence their stability against flocculation or coagulation, whereas a low ζ -potential value indicates that the dispersion tends to collapse leading to flocculation or coagulation. Therefore, ζ values of the vesicles in 3 mM PEGDPC were measured at different pHs. The data are listed in Table S1. The results clearly indicate that at pH 3.0 the surface charge is positive and at pH 10.0 the surface charge is negative, whereas at around pH 6.0–7.0, the surface charge is slightly negative. This means the vesicles are stable in a wide range of pH. Since the zwitterionic vesicles at around neutral pH have tendencies to either grow in size or coagulate producing precipitates, turbidity (τ) measurement of the surfactant solution (3 mM, pH 7.0) was monitored over a period of two months at 400 nm to ensure vesicle stability. However, the plot in Figure S11 shows only a slight increase in turbidity for the surfactant solution and can be attributed to the development of the vesicles. This is supported by the size distribution profiles (Figure S12) of the surfactant solution at different time intervals. The monolayer vesicles in 3 mM PEGDPC solution are found to be highly stable even after two months. The excellent stability of the vesicles makes them potential candidate for drug delivery applications.

To investigate whether there is any effect of salt on the stability of monolayer vesicles, fluorescence anisotropy of DPH in vesicle solution of PEGDPC was measured at different NaCl concentrations. The plot in Figure S13 shows only a slight

increase of r value with the rise of $[NaCl]$. The slight increase of r value of DPH at $[NaCl] = 200$ mM suggests that the monolayer vesicles remain unaffected even in the presence of moderately high salt concentration. The size distribution histogram of 5 mM PEGDPC in the presence of 200 mM NaCl has been depicted as inset in Figure S13. As seen, the size of the monolayer vesicles also remains unaltered even at high NaCl concentration.

4. CONCLUSIONS

In summary, in this work, a novel L-cysteine-derived bolaamphiphile (PEGDPC) with PEG as spacer was developed and characterized. The solution behavior of the amphiphile was investigated in different pHs and temperatures. Despite having so-called polar PEG spacer, the molecule exhibits a reasonably good surface activity in water. Different techniques including fluorescence spectroscopy, DLS, TEM, and AFM confirm formation of monolayer vesicles by the amphiphilic molecules in neutral, acidic, and basic pHs. The surfactant monomers organize themselves to form monolayer vesicle in very dilute as well as in concentrated solution. To the best of our knowledge, this is the first report on vesicle formation by a bolaamphiphile containing PEG as spacer chain. The thermodynamic data suggest that the driving force for vesicle formation is a hydrophobic effect. The monolayer vesicles were observed to be fairly stable with respect to increase of surfactant concentration and temperature. But, the hydrodynamic size of the monolayer vesicles is found to decrease with both decrease and increase of solution pH. The vesicle stability under physiological condition suggests that they can have potential use in drug delivery applications.

■ ASSOCIATED CONTENT

📄 Supporting Information

The Supporting Information is available free of charge on the ACS Publications website at DOI: 10.1021/acs.langmuir.7b01877.

Details of synthetic procedure, FT-IR, 1H NMR, and ^{13}C NMR spectra and chemical identification of the synthesized amphiphiles, representative fluorescence emission spectra of Py, concentration-dependent anisotropy change, MB entrapment, pH-dependent DLS, and HRTEM and cryo-TEM images, salt effect and variation of turbidity with aging (PDF)

■ AUTHOR INFORMATION

Corresponding Author

*Fax (+) 91-3222-255303; e-mail joydey@chem.iitkgp.ernet.in (J.D.).

ORCID

Joykrishna Dey: 0000-0001-8357-5560

Notes

The authors declare no competing financial interest.

■ ACKNOWLEDGMENTS

The authors thank Indian Institute of Technology, Kharagpur, for financial support of this work. We are thankful to Prof. Subhas Chandra Kundu for the DLS and ζ -potential measurements.

■ REFERENCES

- (1) Fuhrhop, H. J.; David, H. H.; Mathieu, J.; Liman, U.; Winter, J. H.; Boekema, E. Bolaamphiphiles and Monolayer Lipid Membranes Made from 1,6,19,24-Tetraoxa-3,21-cyclohexatriacontadiene-2,5,20,23-tetrone. *J. Am. Chem. Soc.* **1986**, *108*, 1785–1791.
- (2) Bohme, P.; Hicke, H.-G.; Boettcher, C.; Fuhrhop, H. J. Reactive and Rigid Monolayers of Bisaroyl Azide Diamide Bolaamphiphiles on Polyacrylonitrile Surfaces. *J. Am. Chem. Soc.* **1995**, *117*, 5824–5828.
- (3) Escamilla, G. H.; Newkome, G. R. Bolaamphiphiles: From Golf Balls to Fibers. *Angew. Chem., Int. Ed. Engl.* **1994**, *33* (19), 1937–1940.
- (4) Fuhrhop, H. J.; Fritsch, D. Bolaamphiphiles Form Ultrathin, Porous and Unsymmetric Monolayer Lipid Membranes. *Acc. Chem. Res.* **1986**, *19* (5), 130–137.
- (5) Mao, G.; Tsao, Y. H.; Tirrell, M.; Davis, T. H.; Hessel, V.; van Esch, J.; Ringsdorf, H. Monolayers of Bolaform Amphiphiles: Influence of Alkyl Chain Length and Counterions. *Langmuir* **1994**, *10* (11), 4174–4184.
- (6) Fuhrhop, H. J.; Wang, T. Bolaamphiphiles. *Chem. Rev.* **2004**, *104*, 2901–2937.
- (7) Kunitake, T.; Okahata, Y. Formation of Stable Monolayer Membranes and Related Structures in Dilute Aqueous Solution from Two-headed Ammonium Amphiphiles. *J. Am. Chem. Soc.* **1979**, *101*, 5231–5234.
- (8) Newkome, R.; Lin, X. F.; Chen, Y. X.; Escamilla, G. H. Two-Directional Cascade Polymer Synthesis: Effects of Core Variation. *J. Org. Chem.* **1993**, *58*, 3123–3129.
- (9) Fuhrhop, H. J.; Spiroski, D.; Boettcher, C. Molecular Monolayer Rods and Tubules Made of α -(L-lysine), ω -(amino) Bolaamphiphiles. *J. Am. Chem. Soc.* **1993**, *115*, 1600–1601.
- (10) Shimizu, T.; Masuda, M. Stereochemical Effect of Even–Odd Connecting Links on Supramolecular Assemblies Made of 1-Glucosamide Bolaamphiphiles. *J. Am. Chem. Soc.* **1997**, *119*, 2812–2818.
- (11) Roussel, M.; Lognone, V.; Plusquellec, D.; Benvegnu, T. Monolayer Lipid Membrane-Forming Dissymmetrical Bolaamphiphiles Derived from Alginate Oligosaccharides. *Chem. Commun.* **2006**, *34*, 3622–3624.
- (12) Guilbot, J.; Benvegnu, T.; Legros, N.; Plusquellec, D.; Dedieu, J.-C.; Gulik, A. Efficient Synthesis of Unsymmetrical Bolaamphiphiles for Spontaneous Formation of Vesicles and Disks with a Transmembrane Organization. *Langmuir* **2001**, *17*, 613–618.
- (13) Shimizu, T.; Iwaura, R.; Masuda, M.; Hanada, T.; Yase, K. Internucleobase-Interaction-Directed Self-Assembly of Nanofibers from Homo- and Heteroditopic 1, ω -Nucleobase Bolaamphiphiles. *J. Am. Chem. Soc.* **2001**, *123*, 5947–5955.
- (14) Iwaura, R.; Yoshida, K.; Masuda, M.; Yase, K.; Shimizu, T. Spontaneous Fiber Formation and Hydrogelation of Nucleotide Bolaamphiphiles. *Chem. Mater.* **2002**, *14*, 3047–3053.
- (15) Yin, S.; Song, B.; Liu, G.; Wang, Z.; Zhang, X. Self-Organization of Polymerizable Bolaamphiphiles Bearing Diacetylene Mesogenic Group. *Langmuir* **2007**, *23*, 5936–5941.
- (16) Kobayashi, H.; Amaike, M.; Jung, J. H.; Friggeri, A.; Shinkai, S.; Reinhoudt, D. N. Organogel or Polymer Gel; Facilitated Gelation of a Sugar-Based Organic Gel by the Addition of a Boronic Acid-Appended Polymer. *Chem. Commun.* **2001**, 1038–1039.
- (17) Shimizu, T.; Kogiso, M.; Masuda, M. Noncovalent Formation of Polyglycine II-Type Structure by Hexagonal Self-Assembly of Linear Polymolecular Chains. *J. Am. Chem. Soc.* **1997**, *119*, 6209–6210.
- (18) Shimizu, T.; Kogiso, M.; Masuda, M. Vesicle Assembly in Microtubes. *Nature* **1996**, *383*, 487–488.
- (19) Claussen, C. R.; Rabatic, M. B.; Stupp, I. S. Aqueous Self-Assembly of Unsymmetric Peptide Bolaamphiphiles into Nanofibers with Hydrophilic Cores and Surfaces. *J. Am. Chem. Soc.* **2003**, *125*, 12680–12681.
- (20) Ambrosi, M.; Fratini, E.; Alfreðsson, V.; Ninham, W. B.; Giorgi, R.; Lo Nostro, P.; Baglioni, P. Nanotubes from a Vitamin C-Based Bolaamphiphile. *J. Am. Chem. Soc.* **2006**, *128* (22), 7209–7214.
- (21) Ray, S.; Das, A. K.; Banerjee, A. Self-Assembly Fibrillar Network Gels of Simple Surfactants in Organic Solvents. *Chem. Mater.* **2007**, *19* (7), 1633–1639.
- (22) Fariya, M.; Jain, A.; Dhawan, V.; Shah, S.; Nagarsenker, S. M. Bolaamphiphiles: A Pharmaceutical Review. *Adv. Pharm. Bull.* **2015**, *4* (2), 483–491.
- (23) Knop, K.; Hoogenboom, R.; Fischer, D.; Schubert, S. U. Poly(ethylene glycol) in Drug Delivery: Pros and Cons as well as Potential Alternatives. *Angew. Chem., Int. Ed.* **2010**, *49*, 6288–6308.
- (24) Svenson, S.; Tomalia, A. D. Dendrimers in Biomedical Applications—Reflections on the Field. *Adv. Drug Delivery Rev.* **2005**, *57*, 2106–2129.
- (25) Tasaki, K. Poly(oxyethylene)–Water Interactions: A Molecular Dynamics Study. *J. Am. Chem. Soc.* **1996**, *118*, 8459–8469.
- (26) Elbert, D. L.; Hubbell, J. A. Surface Treatments of Polymer for Biocompatibility. *Annu. Rev. Mater. Sci.* **1996**, *26*, 365–394.
- (27) Dey, J.; Shrivastava, S. Can Molecules with Anionic Head and Poly(ethylene glycol) methyl ether Tail Self-assemble in Water? A Surface Tension, Fluorescence Probe, Light Scattering, and Transmission Electron Microscopic Investigation. *Soft Matter* **2012**, *8*, 1305–1308.
- (28) Dey, J.; Shrivastava, S. Physicochemical Characterization and Self-Assembly Studies on Cationic Surfactants bearing mPEG Tail. *Langmuir* **2012**, *28*, 17247–17255.
- (29) Ghosh, R.; Dey, J. Vesicle Formation by L-Cysteine-Derived Unconventional Single-Tailed Amphiphiles in Water: A Fluorescence, Microscopy, and Calorimetric Investigation. *Langmuir* **2014**, *30*, 13516–13524.
- (30) Ghosh, R.; Dey, J. Aggregation Behavior of Poly(ethylene glycol) Chain-Containing Anionic Amphiphiles: Thermodynamic, Spectroscopic and Microscopic Studies. *J. Colloid Interface Sci.* **2015**, *451*, 53–62.
- (31) Roy, S.; Mohanty, A.; Dey, J. Microviscosity of Bilayer membranes of some N-Acylamino Acid Surfactants determined by Fluorescence Probe Method. *Chem. Phys. Lett.* **2005**, *414*, 23–27.
- (32) Lakowicz, J. R. *Principles of Fluorescence Spectroscopy*; Plenum Press: New York, 1983; p 132.
- (33) Frisch, M. J.; Trucks, G. W.; Schlegel, H. B.; Scuseria, G. E.; Robb, M. A.; Cheeseman, J. R.; Scalmani, G.; Barone, V.; Mennucci, B.; Petersson, G. A. *Gaussian 09*, revision B.01; Gaussian, Inc.: Wallingford, CT, 2010.
- (34) Rosen, J. M.; Mathias, H. J.; Davenport, L. Aberrant Aggregation Behavior in Cationic Gemini Surfactants Investigated by Surface Tension, Interfacial Tension, and Fluorescence Methods. *Langmuir* **1999**, *15*, 7340–7346.
- (35) Rosen, M.; Li, F.; Morrall, S. W.; Versteeg, D. J. The Relationship between the Interfacial Properties of Surfactants and Their Toxicity to Aquatic Organisms. *Environ. Sci. Technol.* **2001**, *35*, 954–959.
- (36) Ghosh, R.; Dey, J. Vesicle-to-Micelle Transition in Aqueous Solutions of L-Cysteine-Derived Carboxylate Surfactants Containing Both Hydrocarbon and Poly(ethylene glycol) Tails. *Langmuir* **2017**, *33*, 543–552.
- (37) Kalyanasundaram, K.; Thomas, J. K. Environmental Effects on Vibronic Band Intensities in Pyrene Monomer Fluorescence and Their Application in Studies of Micellar Systems. *J. Am. Chem. Soc.* **1977**, *99*, 2039–2044.
- (38) Kalyanasundaram, K. *Photophysics of Microheterogeneous Systems*; Academic Press: New York, 1988.
- (39) Zana, R.; In, M.; Lévy, H.; Duportail, G. Alkanediyl- α,ω -bis(dimethylalkylammonium bromide). 7. Fluorescence Probing Studies of Micelle Micropolarity and Microviscosity. *Langmuir* **1997**, *13*, 5552–5557.
- (40) Laskar, P.; Dey, J.; Ghosh, K. S. Evaluation of Zwitterionic Polymersomes Spontaneously Formed by pH-Sensitive and Biocompatible PEG Based Random Copolymers as Drug Delivery Systems. *Colloids Surf., B* **2016**, *139*, 107–116.
- (41) Tao, W.; Liu, Y.; Jiang, B.; Yu, S.; Huang, W.; Zhou, Y.; Yan, D. A Linear-Hyperbranched Supramolecular Amphiphile and Its Self-

Assembly into Vesicles with Great Ductility. *J. Am. Chem. Soc.* **2012**, *134*, 762–764.

(42) Napoli, A.; Valentini, M.; Tirelli, N.; Muller, M.; Hubbell, A. J. Oxidation-Responsive Polymeric Vesicles. *Nat. Mater.* **2004**, *3*, 183–189.

(43) Garidel, P.; Hildebrand, A.; Neubert, R.; Blume, A. Thermodynamic Characterization of Bile Salt Aggregation as a Function of Temperature and Ionic Strength Using Isothermal Titration Calorimetry. *Langmuir* **2000**, *16*, 5267–5275.

(44) Majhi, P.; Moulik, S. Energetics of Micellization: Reassessment by a High-Sensitivity Titration Microcalorimeter. *Langmuir* **1998**, *14*, 3986–3990.

(45) Bhattacharya, S.; Haldar, J. Thermodynamics of Micellization of Multiheaded Single-Chain Cationic Surfactants. *Langmuir* **2004**, *20*, 7940–7947.